[7]Gallagher, J. A. and Thomas, A.S.W., "Turbulent Boundary Layer Characteristics over Streamwise Grooves," AIAA Paper 84-2185, 1985.
[8]Smith, C. R. and Metzler, S. P., "The Characteristics of Low-Speed Streaks in the Near-Wall Region of a Turbulent Boundary Layer," *Journal of Fluid Mechanics*, Vol. 129, 1983, p. 27.
[9]Doligalski, T. L. and Walker, J.D.A., "The Boundary Layer Induced by a Convected Two-Dimensional Vortex," *Journal of Fluid Mechanics*, Vol. 139, 1984, p. 1.

Observations on the Structure of an Edge-Tone Flowfield

A. Krothapalli*
The Florida State University, Tallahassee, Florida
and
W. C. Horne†
NASA Ames Research Center
Moffett Field, California

Introduction

An edge tone is the sound of a discrete frequency produced by a thin rectangular jet of fluid impinging on a wedge. Edge tones were discovered in 1854 by Sondhaus and have been the subject of a large number of experimental and theoretical investigations. An admirable review of these is given by Karamcheti et al.[1] The wedge is essential to edge-tone generation because the tone does not appear when the wedge is removed from the jet. The nature of the flow processes occurring at the wedge is therefore an important factor in edge-tone production. The interaction region of the flow at the edge has also been used to illustrate the leading-edge "Kutta condition." The detailed features of the unsteady flow at the edge, however, are still to be understood. A discussion of the Kutta condition in unsteady leading-edge flows is given by Crighton,[2] who suggested that the best illustration of such flow is afforded by the edge-tone configuration. With this in mind, an experiment was conducted to examine the unsteady flowfield in the interaction region of the jet with the leading edge of the wedge.

The main parameters or variables governing the problem are the Mach number and Reynolds number of the jet near the exit, the state of the flow at the exit of the nozzle, the geometry and disposition of the wedge with respect to the nozzle exit, and the condition of the ambient medium into which the jet is issuing. The present experiment was conducted in two parts. The first part of the investigation deals with a high-speed subsonic jet ($M=0.8$) impinging on a 20-deg wedge. The second part of the investigation deals with more detailed measurements of the flowfield, using a low-speed subsonic jet ($M=0.23$) impinging again on a 20-deg wedge. The Reynolds number employed was based on the width of the nozzle and was about 5×10^4 for the high-speed case; for the low-speed jet case, it was about 3×10^4. From the measurements of the mean velocity at the nozzle exit, top-hat mean velocity profiles are observed for the two cases tested.

Received Oct. 15, 1985; revision received Dec. 9, 1985.

*Associate Professor, Department of Mechanical Engineering, Florida A&M University/FSU College of Engineering. Member AIAA.
†Aerospace Engineer, Lowspeed Aircraft Research Branch. Member AIAA.

Apparatus, Instrumentation, and Procedure

Experiments described here were conducted at two different times and in two different laboratories. However, when similar parameters were used, both experiments gave similar results. The detailed flow measurements were made using a low-speed jet ($M=0.23$) facility at NASA Ames Research Center. For other measurements, the blowdown facility at Stanford University was used. In the first case, the dimensions of the rectangular exit of the nozzle used were 50 mm long (L) and 3 mm wide (D), and were preceded by a 40-mm-long, smooth, rectangular channel (50 mm × 3 mm). The experimental facility and model are described in detail by Krothapalli and Horne.[3] A 20-deg wedge was selected here because of its use in early Stanford investigations.

A B&K type 4138 microphone (3 mm diam), which has a flat response to about 100 kHz, was used o make the acoustic measurements. The microphone was calibrated using a B&K type 4220 Pistonphone. The location of the microphone was held fixed with respect to the leading edge of the wedge throughout the experiment.

A self-synchronizing schlieren system employing a phase-locked technique was used for flow visualization. The schlieren image of the flowfield was displayed on a ground-glass screen for visual observation or on a film to obtain a photographic record. Schlieren photographs were taken using Polaroid-type 57 instant film (ASA 3000).

The velocity field and surface pressure distribution of a low-speed edge tone were measured at the anechoic chamber facility at Ames Research Center. A rectangular nozzle having dimensions of 0.508 cm × 10.16 cm was used. A 20-deg aluminum wedge was provided with 10 pressure transducer ports and could be positioned at arbitrary distances from the nozzle exit with a lead screw. It was found that multiple nonharmonic tones were generated over most of the operating range of this apparatus. In order to simplify the data sampling procedure, the conditions $M=0.23$ and $h/d=6.25$ were selected for study since only harmonically related tones were observed.

The velocity field was surveyed with a miniature X-wire probe equipped with platinum-coated tungsten sensors 5 μm in diameter and 1 mm long. The probe was operated in the constant temperature mode, which ensured accurate phase response to 3 kHz. Fluctuating surface pressures were measured with 0.48-cm-diam transducers embedded in the wedge and connected to the pressure ports via 0.128-cm-diam passages. The diameter of the pressure port at the surface was 0.064 cm. The intersection of the tip port with the edge produced a 0.064-cm width by 0.02-cm-long notch at the central region of the wedge. All measurements were conditionally sampled on the basis of the phase of one of the surface pressure transducers. A detailed description of the apparatus and procedure is given in Refs. 3 and 4.

Results and Discussion

Flow Visualization

Typical sequences of phase-locked schlieren pictures of the edge-tone flowfield for two different edge heights at an exit Mach number of 0.8 are shown in Fig. 1. The knife edge of the schlieren system is oriented parallel to the jet axis. The signal form the near-field microphone was used to trigger the light source. The wedge in Figs. 1a and 1b is positioned such that the edge tone operates in stage 1 and stage 2 modes, respectively. The time interval between two successive pictures during stage 1 operation is 25 μs, while during stage 2 operation, it is 20 μs. The figure shows the similarity of the overall flowfield for the two cases.

From the sequence of pictures, the following observations are made. Large-scale vortical structures, referred to here as primary vortices, can be identified in the shear layers on either side of the jet, and these grow in intensity as the jet approaches the wedge. At the leading edge, a secondary

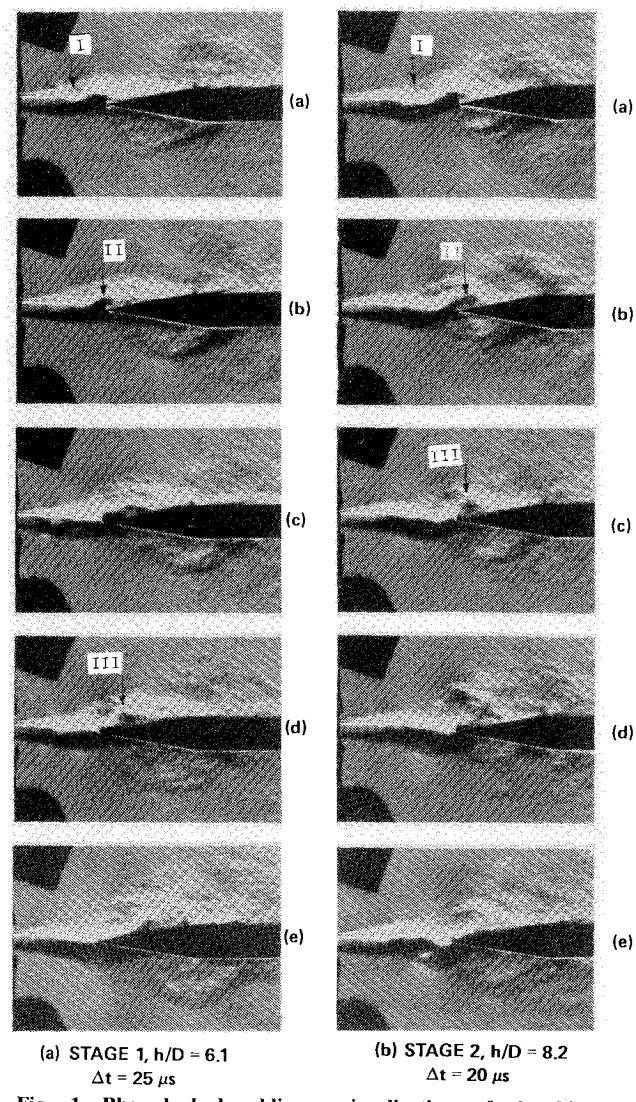

Fig. 1 Phase-locked schlieren visualization of the high-speed ($M=0.8$) edge-tone flowfield, (I) primary or shear-layer, (II) secondary vortex, and (III) counterrotating vortex pair.

vortex arises, with its sign of rotation opposite to that of an oncoming shear layer or primary vortex. Downstream of the tip region, these two vortices form a counter-rotating vortex pair. Eventually they merge and form a single large vortex that moves downstream along the surface of the wedge, as shown in figure. The nature of the primary and secondary vortex formation found here is quite similar to that observed in low-speed ($Re=600$) edge-tone flowfields studied by Rockwell.[5]

From further examination of the details of the pictures, some measure of the local vortex dynamics can be obtained. For example, during the stage 1 operation, the wavelength λ and convection velocity U_c of the primary vortices can be measured and found to be equal to 2.6 cm and 107 m/s, respectively. Corresponding values for stage 2 operation were 1.9 cm and 132 m/s. As a result, the frequency at which primary vortices are created in a given stage was calculated. Respective frequencies for stages 1 and 2 are 4115 and 6947 Hz. These values are close to the amplitude-dominant frequencies obtained from the spectra of the corresponding near-field microphone signals.[3] As expected (based on earlier investigations of low-speed edge tones, that are reviewed by Blake and Powell[6]), the above observation suggests that the primary vortices are shed at a frequency of the dominant tone found in the near sound field. As noted by Karamcheti et al.[1] and Blake and Powell,[6] the convection velocities of

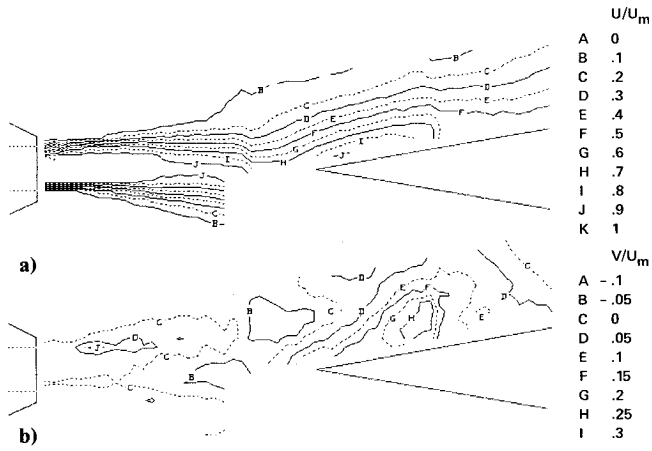

Fig. 2 Typical edge-tone flowfield, $M=0.23$, $h/D=6.25$: a) U component of the velocity; b) V component of the velocity.

the primary vortices are different for different stages. Such an observation is also made here with $U_c/U_0=0.42$ for stage 1 and $U_c/U_0=0.52$ for stage 2, where U_0 is the centerline mean velocity at the nozzle exit.

Another important length scale measured from these pictures was the distance between the adjacent oncoming shear-layer vortex and the secondary vortex at its inception (see the first picture in both stages). During stage 1 operation, this was found to be 0.27 λ_1; the corresponding value for the stage 2 operation is 0.31 λ_2.

Velocity and Surface Pressure Measurements

Because of the relative ease of making the detailed phase-locked measurements in a subsonic jet, both mean velocity and surface pressure data were taken at an exit Mach number of 0.23. However, for fixed geometries of the wedge and the nozzle, the major flow processes show insignificant variation with exit Mach number at least for Mach numbers less than one (see Krothapalli et al.[7]). All the data discussed here are taken at a fixed edge height ($h/d=6.5$).

Typical phase-averaged U and V components of the velocities are shown in Figs. 2a and 2b, respectively. In order to compute vorticity, velocities are normalized with respect to the maximum velocity at the nozzle exit, and the corresponding spatial derivatives are computed using a central difference mesh and are normalized with respect to the nozzle width D. The normalized divergence of the velocity field was computed in order to check the accuracy of the measurements and was found to be less than 0.1 in most of the flow region.

A complete motion cycle of the vorticity field and surface pressure distribution is presented in Figs. 3a and 3b, respectively. Periodic roll-up of the upper shear layer can be observed in Fig. 3a. Also observed are the inception and development of the secondary vortex (which can be identified by the + vorticity, labeled F, in plots 6, 7, 8, and 1 of the figure) in the tip region. From the instantaneous pressure distribution on the upper surface as shown in Fig. 3b, the pressure at the edge is found to be small (with respect to the magnitude of the pressure at other locations). Such an observation is also generally made at the trailing edge of an airfoil placed in an unsteady uniform flow.[8] This seems to indicate that the leading-edge Kutta condition is satisfied at the frequency of the corresponding edge tone. Also shown in the figure are the positive and negative vorticity centers associated with the secondary and primary vorticities, respectively, indicated by the symbols $\oplus$ and $\ominus$. From the amplitude distribution downstream of the tip region, a large positive pressure gradient is observed in plot 3, immediately followed by a positive vorticity center (see plot 4) signifying

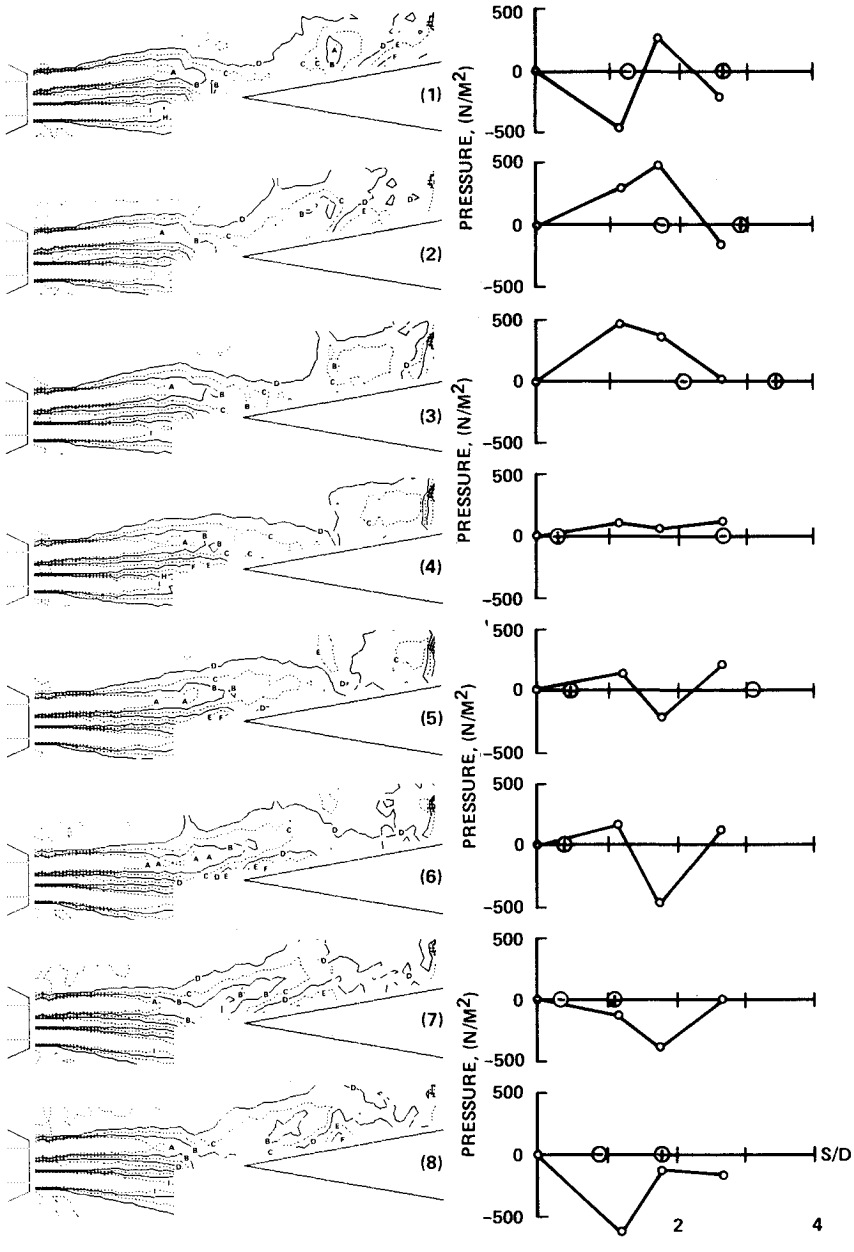

Fig. 3 Phase-averaged vorticity ($\Omega D/U_m$: $A=-1$, $B=-0.75$, $C=-0.5$, $D=-0.25$, $E=0$, $F=0.25$, $G=0.5$, $H=0.75$, $I=1$) and pressure distributions of a low-speed edge-tone flowfield; $M=0.23$; $h/D=6.25$. ⊕, ⊖ are positive and negative vorticity concentrations, respectively.

the formation of the secondary vortex. At this instance, it is interesting to note that the magnitude of the fluctuating pressure is quite small and almost constant along the surface of the wedge.

Conclusions

In this investigation, as mentioned in the introduction, the focus has been on the flow details of the leading-edge region. From the phase-locked flow-visualization pictures of a high-speed jet and conditionally averaged measurements of the velocity, it has been shown that the jet edge interaction gives rise to a secondary vortex at the leading edge in the presence of an established shear layer or primary vortex. These two vortices then form a counterrotating vortex pair and eventually merge into a single large vortex, which moves along the surface of the wedge. These observations are quite similar to those made by Rockwell and his co-workers for low-speed flows.

From the instantaneous pressure distribution on the surface of the wedge, it was found that the amplitude of the unsteady pressure at the leading edge remains small near the leading-edge region for the entire motion cycle. At the trailing edge of an airfoil placed in an unsteady flow, the assumption of zero pressure differential was experimentally verified at low-frequency parameters. Because of the similarities found in the surface pressure distributions near the trailing-edge region of an airfoil and the leading-edge region of the wedge, it may be concluded that the instantaneous zero pressure differential also exists at the leading edge of the wedge.

References

[1]Karamcheti, K., Bauer, A. B., Shields, W. L., Stegen, G. R., and Woolley, J. P., "Some Features of an Edge-Tone Flow Field," NASA SP-207, July 1969.

[2]Crighton, D. G., "Acoustics as a Branch of Fluid Mechanics," *Journal of Fluid Mechanics*, Vol. 106, 1981, pp. 261-298.

[3]Krothapalli, A. and Horne, W. C., "Recent Observations on the Structure of an Edge-Tone Flowfield," AIAA Paper 84-2296, Oct. 1984.
[4]Horne, W. C., "Measurements of Large Scale Disturbances in Rectangular Wall Jets," AIAA Paper 84-2314, Oct. 1984.
[5]Rockwell, D., "Vortex-Edge Interactions," *Recent Advances in Aerodynamics*, edited by A. Krothapalli and C. A. Smith, Springer-Verlag, New York, 1986.
[6]Blake, W. K. and Powell, A., "The Development of Contemporary Views of Flow-Tone Generation," *Recent Advances in Aeroacoustics*, edited by A. Krothapalli and C. A. Smith, Springer-Verlag, New York, 1984.
[7]Krothapalli, A., Karamcheti, K., Hsia, Y., and Baganoff, D., "On Edgetones in Highspeed Flows and Their Application to Multiple Jet Mixing," AIAA Paper 82-0120, Jan. 1982.
[8]Satyanarayana, B., "Unsteady Wake Measurements of Airfoils and Cascades," *AIAA Journal*, Vol. 45, May 1977, pp. 613-618.

Local Equilibrium Assumption for Round Jet Calculations

Ronald M. C. So*
Arizona State University, Tempe, Arizona
and
B. C. Hwang†
David W. Taylor Naval Ship Research and Development Center, Annapolis, Maryland

Introduction

A FAMILY of similarity solutions has been found[1] for self-preserving, incompressible, turbulent round jets. The similarity parameter is $\eta = r/\delta(x)$, where x and r are the axial and radial coordinates, respectively, $\delta(x)$ the jet half-width, defined as the width of the jet at $U/U_0(x) = 0.5$, U is the mean velocity of the jet and U_0 is the jet centerline velocity. All memebers of the family lead to power-law decay for δ and $U_0(x)$, namely $\delta \alpha x$ and $U_0 \alpha x^{-1}$; however, they differ in the behavior of the eddy viscosity, ν_t. The classical Tollmien[2] solution is given by constant ν_t. Other similarity solutions are also possible depending on the variation of $\nu_t(\eta)$. Some of these solutions are not physically valid, even though they are similarity solutions to the jet governing equations, because they lead to zero ν_t at the jet centerline. One member among those that give rise to finite $\nu_t(0)$ is found to give better agreement with the mean and turbulent flux measurements of Wygnanski and Fiedler[3] and Chevray and Tutu[4] than the classical Tollmien[2] solution. Since ν_t decreases from $\nu_t(0)$ to zero as $\eta \to \infty$, it is more realistic than constant ν_t and is in better quantitative agreement with measured ν_t.

The purpose of this Note is to make use of these similarity solutions to obtain closed-form similarity solutions to the k and ϵ equations and, in the process, assess the influence of the local equilibrium assumption on round jet calculations. These closed-form solutions will be compared with the numerical similarity solution obtained by Vollmers and Rotta[5] using a k-kl closure model and the k-ϵ model calculation of Launder et al.[6] It will be shown that while the neglect of the equilibrium assumption leads to a decay of the centerline turbulent kinetic energy, k_0, as x^{-2}, the asumption gives a decay of x^{-1}. The latter result seems to be in better quantitative agreement with measurements.

Received April 16, 1985; revision submitted Dec. 20, 1985.

*Professor, Mechanical and Aerospace Engineering Department.
†Research Scientist.

Analysis

Transport of turbulent kinetic energy k and the dissipation rate of k, ϵ, in an incompressible round jet is governed by the equations[6]

$$U\frac{\partial k}{\partial x} + V\frac{\partial k}{\partial r} = \frac{1}{r}\frac{\partial}{\partial r}\left(\frac{r\nu_t}{\sigma_k}\frac{\partial k}{\partial r}\right) + \nu_t\left(\frac{\partial u}{\partial r}\right)^2 - \epsilon \tag{1}$$

$$U\frac{\partial \epsilon}{\partial x} + V\frac{\partial \epsilon}{\partial r} = \frac{1}{r}\frac{\partial}{\partial r}\left(\frac{r\nu_t}{\sigma_\epsilon}\frac{\partial \epsilon}{\partial r}\right) + C_{\epsilon 1}\frac{\epsilon}{k}\nu_t\left(\frac{\partial U}{\partial r}\right)^2 - C_{\epsilon 2}\frac{\epsilon^2}{k} \tag{2}$$

where U and V are the mean velocities along x and r, respectively, σ_k and σ_ϵ are the Prandtl numbers for k and ϵ, and $C_{\epsilon 1}$ and $C_{\epsilon 2}$ are model constants. The values assumed by Launder et al.[6] for σ_k, σ_ϵ, $C_{\epsilon 1}$, and $C_{\epsilon 2}$ are 1, 1.3, 1.9, and 1.4, respectively. The boundary conditions for k and ϵ are $k(x,0) = k_0(x)$, $k(x,\infty) = 0$, $\epsilon(x,0) = \epsilon_0(x)$, and $\epsilon(x,\infty) = 0$, where $k_0(x)$ and $\epsilon_0(x)$ are centerline values of k and ϵ and have to be determined as part of the solutions. If the local equilibrium assumption or production of k balances the dissipation of k is made; Eqs. (1) and (2) are then reduced to forms similar to the mean momentum equation for round jets. This suggests that Eqs. (1) and (2) can be analyzed in the manner suggested by So and Hwang.[1] Here, only the most valid solution is used to analyze Eqs. (1) and (2). According to Ref. 1, that solution is given by

$$U = U_0 e^{-\eta^2 \ell n 2} \tag{3}$$

$$V = \frac{4U_0(\ell n 2)^2}{Re_t}\left[\eta e^{-\eta^2 \ell n 2} + \frac{e^{-\eta^2 \ell n 2} - 1}{2\eta \ell n 2}\right] \tag{4}$$

$$\frac{\nu_t}{\nu_t(0)} = \frac{1 - e^{-\eta^2 \ell n 2}}{\eta^2 \ell n 2} \tag{5}$$

$$\delta' = \frac{4(\ell n 2)^2}{Re_t} \tag{6}$$

$$\frac{U_0'}{U_0} = -\frac{\delta'}{\delta} \tag{7}$$

where $Re_t = [U_0\delta/\nu_t(0)]\ell n 2$, the turbulent Reynolds number, is taken to be constant and is determined from jet spread, the primes denote differentiation with respect to x. Substituting Eqs. (3-7) into Eqs. (1) and (2), invoking the assumption $\nu_t(\partial U/\partial r)^2 = \epsilon$, and making use of the boundary conditions, the following solutions for k and ϵ are obtained:

$$\frac{k}{k_0} = \frac{\epsilon}{\epsilon_0} = e^{-\eta^2 \sigma_k \ell n 2} \tag{8}$$

$$\frac{k_0'}{k_0} = -\frac{\delta'}{\delta} \tag{9}$$

$$\frac{\delta\epsilon_0'}{\epsilon_0} = -\frac{4(\ell n 2)^2 \sigma_k}{\sigma_\epsilon Re_t}(1 + \sigma_k - \sigma_\epsilon) \tag{10}$$

$$\frac{1}{\sigma_\epsilon} = \frac{1}{\sigma_k} + \frac{Re_t(C_{\epsilon 2} - C_{\epsilon 1})}{4(\ell n 2)^2 \sigma_k^2}\frac{\delta\epsilon_0}{k_0 U_0} \tag{11}$$

With the results, $\delta \alpha x$ and $U_0 \alpha x^{-1}$ from Eqs. (6) and (7), the decay of k_0 and ϵ_0 can be deduced from Eqs. (9) and (10) to be $k_0 \alpha x^{-1}$ and $\epsilon_0 \alpha x^{-3}$. Equation (11) gives a relation for the determination of σ_ϵ once Re_t, σ_k, $C_{\epsilon 1}$, and $C_{\epsilon 2}$ are specified. On the other hand, a similarity solution for k (even though